

Characterization of epitaxial growth of Fe(1 1 0) on (1 1 –2 0) sapphire substrates driven by Mo(1 1 0) seed layers

U. May, R. Calarco ^{*}, J.O. Hauch, H. Kittur, M. Fonine, U. Rüdiger, G. Güntherodt

II. Physikalisches Institut, RWTH Aachen, 52056 Aachen, Germany

Abstract

The molecular beam epitaxy (MBE) growth of bcc Fe(1 1 0) thin films on an Al₂O₃(1 1 –2 0) substrate using Mo(1 1 0) seed layers has been investigated. The growth was studied by reflection high energy electron diffraction (RHEED) in reciprocal space as well as by scanning tunneling microscopy in real space. The relative orientation between the lattices of the Fe(1 1 0) layer and the Al₂O₃(1 1 –2 0) substrate has been identified and has enabled the construction of a model of the in-plane atomic arrangements. Side reflections found in RHEED patterns indicate the formation of ordered relaxation lines along the [1 0 0] direction of the Fe(1 1 0).

Keywords: Reflection high-energy electron diffraction (RHEED); Molecular beam epitaxy; Scanning tunneling microscopy; Epitaxy; Growth; Iron; Molybdenum; Metallic surfaces

1. Introduction

Since the discovery of the giant magnetoresistance (GMR) in magnetic multilayers [1,2] the research in the field of magnetoelectronics has been particularly active. Magnetic tunnel junctions (MTJs) have attracted increasing interest in recent years [3–6] for their applications in magnetic field sensors [7,8] and non-volatile magnetic random access memory (MRAM) [5,9,10]. Strong effort has been focused on the fabrication of junctions with reproducible characteristics and signifi-

cant changes in the magnetoresistance at room temperature [3,5]. High values of tunneling magnetoresistance (TMR) can be achieved if the ferromagnetic electrodes have a high spin polarization [11] and a smooth surface that results in a sharp electrode/barrier interface. For this demand the growth of highly spin-polarized ferromagnetic materials on insulating as well as semiconducting substrates has to be investigated.

In this article we present detailed studies of the growth of epitaxial bcc Fe(1 1 0) with a Mo seed layer on insulating Al₂O₃(1 1 –2 0) substrates. The (1 1 0) orientation of bcc Fe exhibits a high negative spin polarization of –80% at the Fermi energy E_F in spin-polarized photoemission [12,13]. Therefore it can be suitable as ferromagnetic electrode material in MTJs. Moreover, it can be oxidized into Fe₃O₄ (1 1 1) [14,15], which exhibits also a

^{*} Corresponding author. Tel.: +49-241-80-4486/7122; fax: +49-241-88-88306.

E-mail address: calarco@physik.rwth-aachen.de (R. Calarco).

spin polarization of -80% at E_F [16]. It remains to be tested whether Fe(110) or Fe₃O₄(111) yields the better interface to the oxide tunnel barrier.

For epitaxial bcc Fe(110) thin films grown on Al₂O₃(11-20) substrates using a Mo buffer it was already shown that the film demagnetization factors confine the magnetization to the (110) plane [17]. In addition to the cubic magnetocrystalline anisotropy the Fe(110) plane has a strong in-plane strain induced uniaxial anisotropy component along the [001] direction. Along the [001] direction the cubic and uniaxial anisotropy constants have been determined to $K_1 = 6.3 \times 10^5$ erg/cm³ and $K_u = 3.0 \times 10^5$ erg/cm³, respectively [17].

The films were grown by molecular beam epitaxy (MBE) which allows the controlled thin film growth with sub-monolayer precision and high material purity. The details of the growth have already been discussed [18,19]. It was found experimentally that the growth of Fe on Mo single crystals follows a Stranski–Krastranov mode instead of the Frank–Van-der-Merwe mode expected on the basis of surface energy arguments [20–22]. Flat surfaces can be obtained for a growth at a temperature of 600 K [23]. They are also obtained at a low temperature growth (380 K) with successive annealing [24]. In order to reduce in-plane twinning of crystallites and mosaicity, the Mo seed layer has to be deposited at temperatures as high as possible (up to 1060 K) [25,26].

2. Experimental details

The experiments were performed in an UHV system (base pressure 8×10^{-11} mbar), which consists of different interconnected chambers equipped with a MBE facility containing four Knudsen cells and two electron-beam evaporators. Reflection high energy electron diffractometry (RHEED) with a computer-controlled CCD camera is available to follow the layer-by-layer growth. RHEED patterns are acquired at a beam energy of 35 keV and an incidence angle of $<5^\circ$. The surface analysis can be performed via Auger electron spectroscopy (AES), X-ray photoelectron spectroscopy (XPS), low energy electron diffraction (LEED), and scanning tunneling microscopy (STM). The

STM consists of a modified Besocke-type [27] microscope, with a piezoelectric tube of maximum scanning area of 555×555 nm² and lateral resolution of ± 0.1 Å. Tungsten tips for the STM have been prepared by wet chemical etching (in a NaOH solution) and in situ sputtering using Ar ions.

Al₂O₃ substrates with a (11-20) orientation have been used, which were cut with two parallel edges 35° off the in-plane [0001] direction to align the [001] easy axis of (110) oriented Fe films along these edges of the substrate. Both materials, Mo and Fe, were deposited by electron-beam evaporation with a growth rate ranging between 0.03 and 0.06 Å/s. The substrate temperature during the Mo deposition has been adjusted to 840 K and then reduced to 610 K for the Fe growth. The temperature of the samples was controlled within an error of ± 10 K by a NiCr–Ni thermocouple connected to the sample holder. The layer thickness was measured with a calibrated quartz micro-balance within an accuracy of ± 0.5 Å.

3. Results and discussion

The growth of the samples was investigated by RHEED performed with the incident electron beam in different directions: perpendicular to the in-plane [0001] direction (*c*-axis) of the substrate, parallel to [001] direction (magnetic easy axis) of the Fe(110) film, and parallel to the [1-10] direction of the Fe(110) film.

As a result of this experiment it is possible to visualize the in-plane relationship of the crystal lattices involved (see Fig. 1). It has to be noted that all three RHEED experiments are necessary to provide a unique orientation of the Mo(110) and Fe(110) layers on the substrate surface and to exclude the possibility of another configuration mirrored in respect to the [1-12] direction. In this model strain and relaxation factors are not taken into account. The lattice mismatch between Mo and Fe is 8.7% inducing a strained growth in the first layer with a subsequent relaxation due to formation of dislocations. For this schematic growth model all layers are considered with their bulk lattice parameters. In Fig. 1 the magnetic easy

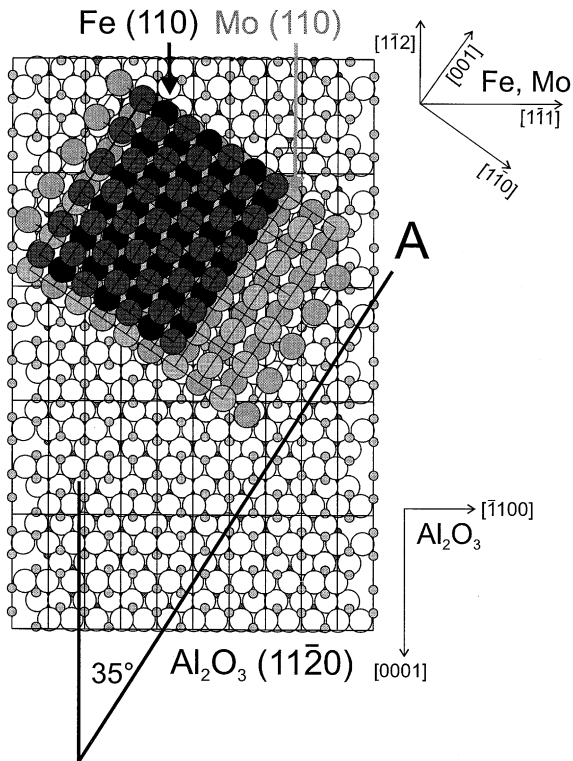


Fig. 1. Schematic model of the in-plane orientation of a Fe(110)/Mo(110)/Al₂O₃(11-20) multilayer. The [1-1] direction of the Mo and Fe layer is parallel to [-1100] direction of the substrate, while the magnetic easy axis of the Fe along the [001] direction is marked by the bold line labeled A. (Open spheres are O atoms, shaded small spheres are Al atoms).

axis of Fe is shown by a solid line labeled A. The oxygen atoms of the substrate are arranged right along this axis, so that they provide a good base for the epitaxial growth of Mo.

The first RHEED study was performed during the deposition of the Mo layer with the incident electron beam perpendicular to the in-plane [0001] substrate direction. The RHEED patterns of the clean Al₂O₃(11-20) substrate, covered with 2.25, 10.5 and 50 monolayers (ML) of Mo are shown in Fig. 2(a)–(d), respectively. Comparing Fig. 2(a) and (b) it can be noticed that the change of the diffraction features from pure substrate spots to the bcc-like structure of Mo appears during the deposition of the first few monolayers. The change of the structure is a non-gradual pro-

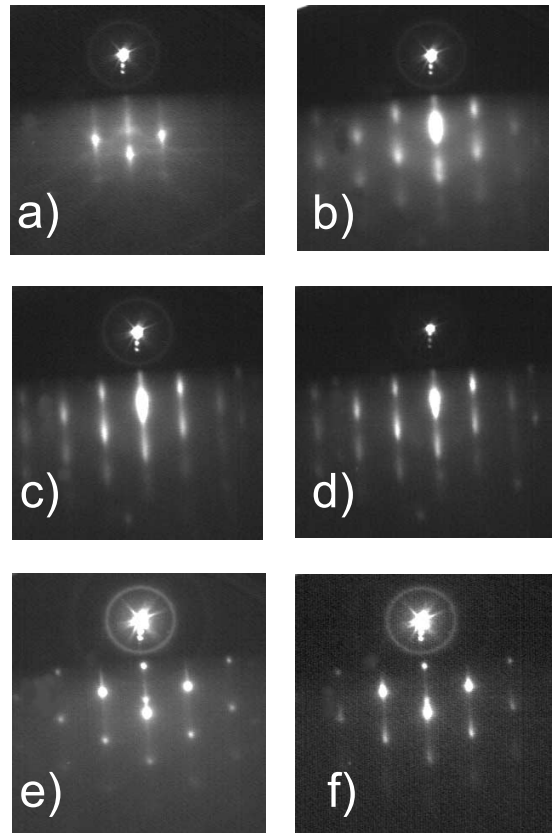


Fig. 2. RHEED pattern with the incident electron beam perpendicular to the [0001] direction of the substrate of (a) the pure Al₂O₃(11-20) substrate, (b) 2.25 ML of Mo (c) 10.5 ML of Mo, (d) 50 ML of Mo grown at 840 K, as well as (e) 10 ML of Fe and (f) 150 ML of Fe grown on 50 ML of Mo at 610 K. Mo has a bcc unit cell and grows (110) oriented with the in-plane [1-1] direction orthogonal to the [0001] direction of the substrate.

cess as expected for a pseudomorphic growth regime followed by lattice relaxations. This can be described by a continuous disappearance of the reflections of the substrate and an appearance of the reflections of the film. Once the Mo structure is established after a few monolayers there are no significant changes in the pattern for increasing Mo thickness indicating that there is no further relaxation of the lattice. However, the RHEED reflexes in Fig. 2(b)–(d) tend to get elongated suggesting the formation of wider 2D terraces. We can clearly identify a Mo [1-1] direction from

the hexagonal structure of the pattern. Therefore, the Mo arranges itself to grow with the $[1\bar{1}1]$ direction perpendicular to the in-plane $[0001]$ direction of the sapphire substrate.

In order to determine the surface topography in real space STM experiments were performed. The STM image of 50 ML Mo on an $\text{Al}_2\text{O}_3(11\bar{2}0)$ substrate (Fig. 3) on a scale of $220 \times 220 \text{ nm}^2$ gives a view of non-ordered islands with a peak-to-peak roughness of $\approx 10 \text{ \AA}$. Locally there is a formation of small islands with an averaged diameter of 20 nm.

Fig. 2(e) and (f) show RHEED patterns of 10.5 and 150 ML of Fe, respectively, grown on the Mo seed layer. Fe has also a bcc unit cell as Mo and it grows also (110) oriented with the $[1\bar{1}1]$ direction orthogonal to the c -axis of the substrate. During deposition the crossover from the Mo RHEED spots to the Fe spots is completed after a few monolayers. As observed for Mo/ Al_2O_3 we find no regime of pseudomorphic strained growth of Fe. Once established the Fe structure does not change significantly until the appearance of side reflections (see below).

Fig. 4 shows a STM image of a 125 ML thick Fe layer. The shape of the islands shows an anisotropic growth of Fe terraces with a preferential growth direction well known for metal growth in

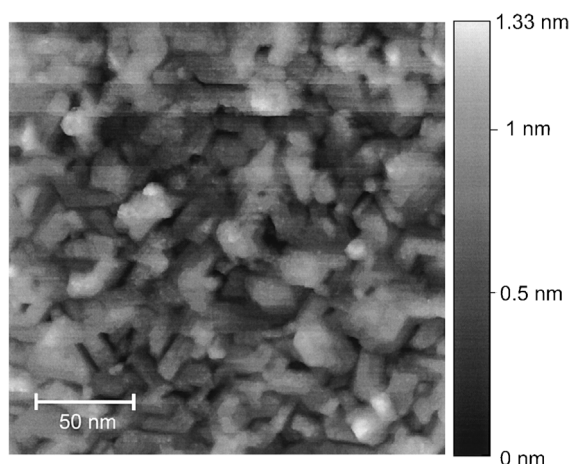


Fig. 3. The STM image of Mo (50 ML)/ $\text{Al}_2\text{O}_3(11\bar{2}0)$ shows non-ordered small islands with an averaged size of $20 \times 20 \text{ nm}^2$ and a peak-to-peak roughness of 10 Å.

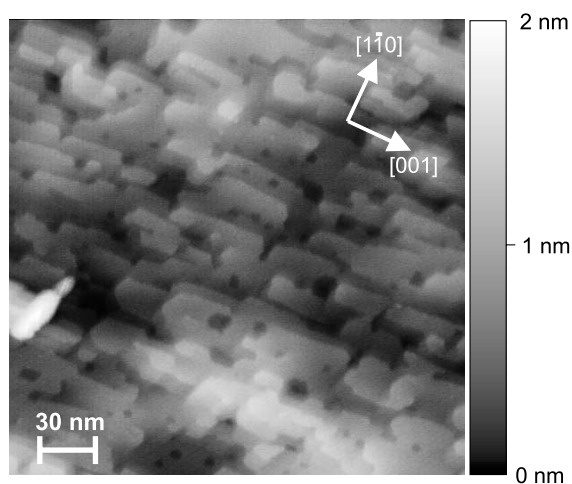


Fig. 4. STM image of the Fe/Mo (50 ML)/ $\text{Al}_2\text{O}_3(11\bar{2}0)$ surface after deposition of 125 ML of Fe.

(110) orientation. The long axis of the islands is parallel to the $[001]$ direction. On the scale of $227 \times 227 \text{ nm}^2$ approximately 10 open layers are visible indicating a multi-terrace growth.

The second RHEED experiment was performed with the incident electron beam parallel to the Fe $[001]$ direction (magnetic easy axis of the Fe (110)), which is around 35° off the c -axis of the substrate. The evolution of the Fe growth has been investigated by analyzing the RHEED patterns as function of Fe layer thickness (Fig. 5). The RHEED image of the substrate is shown in (a) while the images (b) and (c) correspond to 3.8 and 50 ML of Mo, respectively. Also in Fig. 5 the RHEED patterns of (d) 2.7 ML, (e) 58 ML, and (f) 105 ML of Fe are shown. The rectangle-like RHEED patterns of the (110) oriented Mo and Fe layers confirms that the incident electron beam is parallel to the $[001]$ direction of the Mo and Fe layer. Similar to the experiment with the incident electron beam along the $[1\bar{1}1]$ direction we found no regimes of strained pseudomorphic growth neither for the growth of Mo nor of Fe.

In Fig. 5(f) (105 ML of Fe) a set of less intense streaks is visible beside the main streaks. These reflexes appear at a thickness of approximately 25 ML of Fe near one-fifth of the $(00)-(10)$ streaks distance. An explanation of these features could be

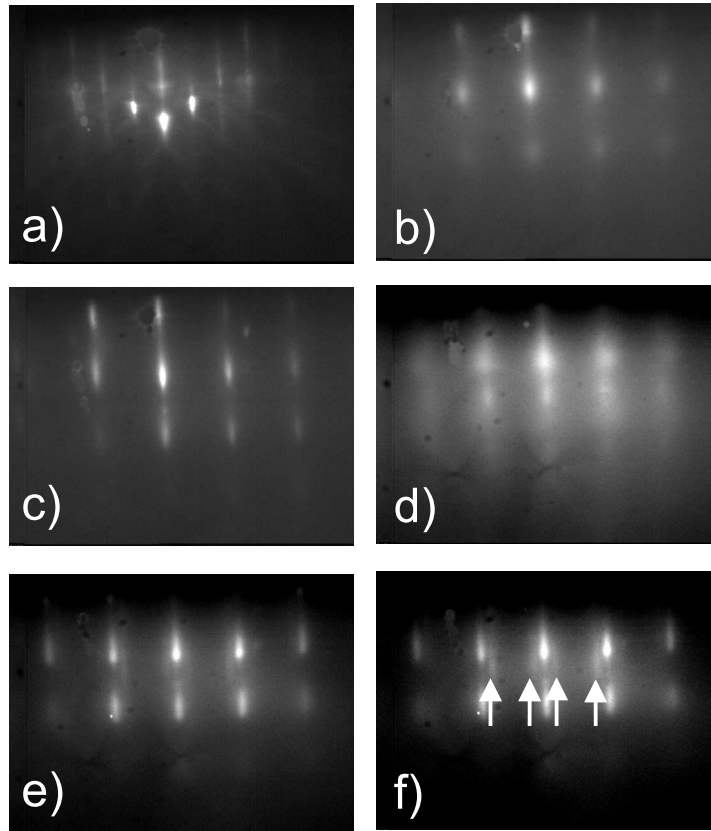


Fig. 5. RHEED pattern with the incident electron beam parallel to the Fe $[001]$ direction 35° off the $[0001]$ direction of the substrate of (a) the pure $\text{Al}_2\text{O}_3(11-20)$ substrate, (b) 3.8 ML of Mo, (c) 50 ML of Mo on an $\text{Al}_2\text{O}_3(11-20)$ substrate, (d) 2.7 ML of Fe, (e) 58 ML Fe, and (f) 105 ML Fe on Mo (50 ML)/ $\text{Al}_2\text{O}_3(11-20)$.

the formation of faceting [28], but the typical reflexes due to a faceting pattern usually lie along directions with different angular orientations with respect to the line through the main reflections. In addition, the Fe surface (Fig. 4) is relatively flat and does not show large step heights of the islands, which usually are the origin of facet reflections if oriented along a high symmetry direction. Another explanation could be the formation of relaxation lines following a high symmetry direction on the surface, because the side reflections appear only when we consider the direction parallel to the $[001]$ direction of Fe (along $[1-10]$ Fe and $[1-11]$ Fe these side reflections are not visible). Since the reflexes (Fig. 5(f)) are located at about one-fifth of the distance between the main reflections, this corresponds to a distance between re-

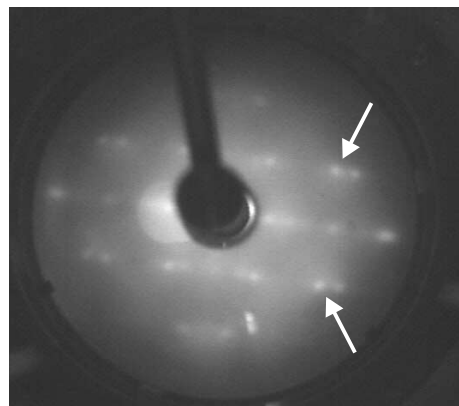


Fig. 6. LEED pattern of Fe(112 ML)/Mo(50 ML)/ $\text{Al}_2\text{O}_3(11-20)$ at an electron energy of 291 eV. The arrows indicate the side reflexes corresponding to a lattice deformation along the $[100]$ direction.

laxation lines of roughly 14 \AA . Such a (5×1) superstructure can be formed by an anisotropic strain relaxation on the surface resulting in an ordered relaxation pattern with dislocation lines parallel to the $[100]$ direction of the Fe. Clemens et al. [29] showed by grazing angle X-ray diffraction that the strain along the $[001]$ direction is released slower than in the $[1-10]$ direction and can therefore be the origin for ordered relaxation. This could lead to relaxation lines parallel to $[100]$ Fe. We have performed LEED measurements to confirm the RHEED results and to study the relaxation lines along the $[100]$ direction in more detail. In Fig. 6 a LEED pattern of a sample with 112 ML of Fe is shown. The LEED pattern shows the presence of side reflections, which correspond to a lattice distortion ($1/5$ of the Fe lattice pa-

rameter) in the $[100]$ direction. Similar relaxation-line induced superstructures were also found by Gradmann et al. (2 ML of Fe on W, deposition at 500 K) [30] and by Tikhov et al. (20 ML of Fe on Mo, deposition at room temperature) [18].

The Fe surface has also been investigated by STM at different thicknesses. For a coverage of 10 ML ($\approx 20 \text{ \AA}$) the images show a surface of flat islands growing one on top of the other. A typical image is shown in Fig. 7. In this image the presence of lines following the perimeter of the islands can be noticed. The height contrast of these lines is less than 1 ML. We address them as relaxation lines caused by misfit dislocations generated to release the strain in the Fe film. These contour lines are spaced by 37 \AA . The STM images show relaxation lines at a lower thickness than observed in the

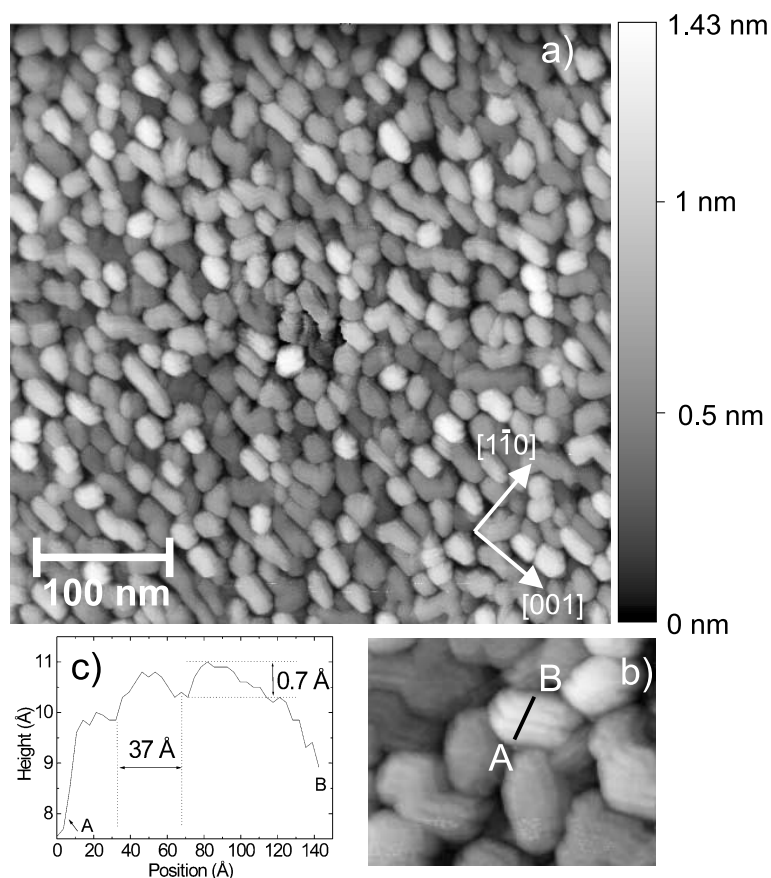


Fig. 7. (a) STM image of the surface of Fe(10 ML)/Mo(50 ML)/ $\text{Al}_2\text{O}_3(11-20)$, (b) relaxation lines appearing as island contour lines with a periodicity of 37 \AA , and (c) the height contrast of relaxation lines of less than one atomic layer as shown in the line profile.

RHEED pattern (Fig. 5(f)). Also a discrepancy in the spacing between the lines was found (larger for STM than for RHEED). This could be due to the presence of some residual strain not completely released in the low-thickness regime. For higher thicknesses additional relaxation lines can lead to a more dense packing of lines. In the STM images (Fig. 7) it is clearly visible that the strain relaxation is anisotropic and develops in lines along the long axis ([001] direction) of the islands. For thicknesses of 1 ML Fe/Mo(110) Malzbender et al. [19] also showed that the long axis of the islands is along the [001] direction, which is consistent with our results.

4. Conclusions

We have studied the epitaxial growth of Fe(110) on a Mo(110) seed layer deposited on a (11-20) oriented sapphire substrate. The interpretation of the RHEED pattern leads to a schematic model of the in-plane symmetry of the (110) oriented Mo and Fe layers on $\text{Al}_2\text{O}_3(11-20)$ substrates without considering relaxations. From the analysis of the RHEED pattern we could identify the presence of side reflections not due to facetting features. These secondary reflexes can be explained on the basis of relaxation line formation along the [100] direction of the Fe. By means of STM imaging at a coverage of 10 ML Fe we found relaxation lines (step distance of 37 Å and a height less than an atomic layer) following the contour of the islands.

Acknowledgements

This work was supported by the German Federal Ministry for Education and Research "BMBF" under grant no. FKZ 13N7329 and the EC TMR Program "Submicron Magnetic Structures and Magneto-Transport Devices" (SUBMAGDEV).

References

- [1] M.N. Baibich, J.M. Broto, A. Fert, F. Nguyen Van Dau, F. Petroff, P. Etienne, G. Creuzet, A. Friederich, J. Chazelas, *Phys. Rev. Lett.* 61 (1988) 2472.
- [2] G. Binasch, P. Grünberg, F. Saurenbach, W. Zinn, *Phys. Rev. B* 39 (1989) 4828.
- [3] J.S. Moodera, L.R. Kinder, T.M. Wong, R. Merservey, *Phys. Rev. Lett.* 74 (1995) 3273.
- [4] T. Yaoi, S. Ishio, T. Miyazaki, *J. Mag. Mag. Mater.* 126 (1993) 430.
- [5] W.J. Gallagher, et al., *J. Appl. Phys.* 81 (1997) 3741.
- [6] J. Nassar, M. Hehn, A. Vaures, F. Petroff, A. Fert, *Appl. Phys. Lett.* 73 (1998) 698.
- [7] M. Sato, H. Kikuchi, K. Kobayashi, *J. Appl. Phys.* 83 (1998) 6691.
- [8] M. Tondra, J.M. Daughton, D. Wang, R.S. Beech, A. Fink, J.A. Taylor, *J. Appl. Phys.* 83 (1998) 6688.
- [9] J.M. Daughton, *J. Appl. Phys.* 81 (1997) 3758.
- [10] H. Boeve, R.J.M. van der Veerdonk, B. Dutta, J. de Boeck, J.S. Moodera, G. Borghs, *J. Appl. Phys.* 83 (1998) 6700.
- [11] M. Julliere, *Phys. Lett.* 54A (1975) 225.
- [12] W. Weber, D.A. Wesner, G. Güntherodt, U. Linke, *Phys. Rev. Lett.* 66 (1991) 942.
- [13] J. Callaway, C.S. Wang, *Phys. Rev. B* 16 (1977) 2095.
- [14] H.-J. Kim, J.-H. Park, E. Vescovo, *Phys. Rev B* 61 (2000) 15284.
- [15] H.-J. Kim, J.-H. Park, E. Vescovo, *Phys. Rev B* 61 (2000) 15288.
- [16] Y. Dedkov, U. Rüdiger, G. Güntherodt, *Phys. Rev. Lett.*, submitted for publication.
- [17] J. Yu, U. Rüdiger, A. Kent, L. Thomas, S.S.P. Parkin, *Phys. Rev. B* 60 (1999) 7352.
- [18] M. Tikhov, E. Bauer, *Surf. Sci.* 232 (1990) 73.
- [19] J. Malzbender, M. Przybylski, J. Giergiel, J. Kirschner, *Surf. Sci.* 414 (1998) 187.
- [20] H.J. Elmers, U. Gradmann, *Appl. Phys. A* 51 (1990) 255.
- [21] L.Z. Mezey, J. Giber, *Jpn. J. Appl. Phys.* 21 (1982) 1569.
- [22] L. Vitos, A.V. Ruban, H.L. Skriver, J. Kolla, *Surf. Sci.* 411 (1998) 186.
- [23] M. Albrecht, H. Fritzsche, U. Gradmann, *Surf. Sci.* 294 (1993) 1.
- [24] O. Fruchart, J.P. Nozieres, D. Givord, *J. Magn. Magn. Mater.* 207 (1999) 158.
- [25] Y. Igarashi, M. Kanayama, *J. Appl. Phys.* 52 (1981) 7208.
- [26] A. Gibaud, et al., *Phys. Rev. B* 48 (1993) 14463.
- [27] K. Besocke, *Surf. Sci.* 181 (1987) 145.
- [28] O. Fruchart, S. Jaren, J. Rothman, *Appl. Surf. Sci.* 135 (1998) 218.
- [29] B.M. Clemens, R. Osgood, A.P. Payne, B.M. Lairson, S. Brennan, R.L. White, W.D. Nix, *J. Magn. Magn. Mater.* 121 (1993) 37.
- [30] U. Gradmann, G. Waller, *Surf. Sci.* 116 (1982) 539.